tion of a genuine patterning process that can be observed in very different developmental situations, including those found in *Drosophila* itself.

But the stripes on the fish still call for more explanation: those shown in Figure 1 of the paper by Kondo and Asai [1] are very narrow with respect to the spaces in between. All the models I know of can only produce stripes and interstripes of the same size.

REFERENCES

1. S. Kondo & R. Asai, *Nature* **376**, 765 (1995).
2. P. W. Ingham & A. Martinez-Arias, *Cell* **68**, 221 (1992).
3. M. Akam, *Nature* **341**, 282 (1989).
4. S. Roth & T. Schupbach, *Development* **120**, 2245 (1994).
5. R. J. Sommer & D. Tautz, *Nature* **361**, 448 (1993).
6. N. H. Patel, B. G. Condron & K. Zinn, *Nature* **367**, 429 (1994).
7. M. Frasch, T. Hoey, C. Rushlow, H. Doyle & M. Levine, *EMBO J.* **6**, 749 (1987).
8. A. M. Turing, *Phil. Trans. R. Soc.* **B237**, 37 (1952).
9. A. Gierer & H. Meinhardt, *Kybernetik* **12**, 30 (1972).
10. V. Castets, E. Dulos, J. Boissonade & P. De Kepper, *Phys. Rev. Lett.* **64**, 2953 (1990).
11. Q. Ouyang & H. L. Swinney, *Nature* **352**, 610 (1991).
12. M. J. Lyons & L. G. Harrison, *Dev. Dynamics* **195**, 201 (1992).
13. H. Meinhardt, *Development* (suppl.) 169 (1989).
14. H. Meinhardt & A. Gierer, *J. Theor. Biol.* **85**, 429 (1980).
15. S. Baumgartner, D. Martin, C. Hagios & R. Chiquet-Ehrismann, *EMBO J.* **13**, 3728 (1994).
16. J. F. Colas, J. M. Launay, O. Kellermann, P. Rosay & L. Maroteaux, *Proc. Natn. Acad. Sci. U.S.A.* **92**, 5441 (1995).

A Reaction-Diffusion Wave on the Skin of the Marine Angelfish Pomacanthus

Nature, **376** (1995) 765–768.

Shigeru Kondo, Rihito Asai

In 1952, Turing proposed a hypothetical molecular mechanism, called the reaction-diffusion system [1], which can develop periodic patterns from an initially homogeneous state. Many theoretical models based on reaction-diffusion have been proposed to account for patterning phenomena in morphogenesis [2–4], but, as yet, there is no conclusive experimental evidence for the existence of such a system in the field of biology [5–8]. The marine angelfish, *Pomacanthus*, has stripe patterns which are not fixed in their skin. Unlike mammal skin patterns, which simply enlarge proportionally during their body growth, the stripes of *Pomacanthus* maintain the spaces between the lines by the continuous rearrangement of the patterns. Although the pattern alteration varies depending on the conformation of the stripes, a simulation program based on a Turing system can correctly predict future patterns. The striking similarity between the actual and simulated pattern rearrangement strongly suggests that a reaction-diffusion wave is a viable mechanism for the stripe pattern of *Pomacanthus*.

When juveniles of *Pomacanthus semicirculatus* are smaller than 2 cm long, they have only three dorsoventral stripes (Figure 1(a)). As they grow, the intervals of the stripes get wider proportionally until the body length reaches 4 cm. At that stage, new stripes emerge between the original stripes (Figure 1(b)). As a result, all the spaces between the stripes revert to that of the 2-cm juvenile. New lines are thin at first, but gradually get broader. When the body length reaches 8–9 cm, an identical process is repeated (Figure 1(c)).

Author affiliations: S. Kondo: Kyoto University Centre for Molecular Biology and Genetics, Kyoto, Japan. R. Asai: Kyoto University Seto Marine Biological Laboratory, Wakayama, Japan.

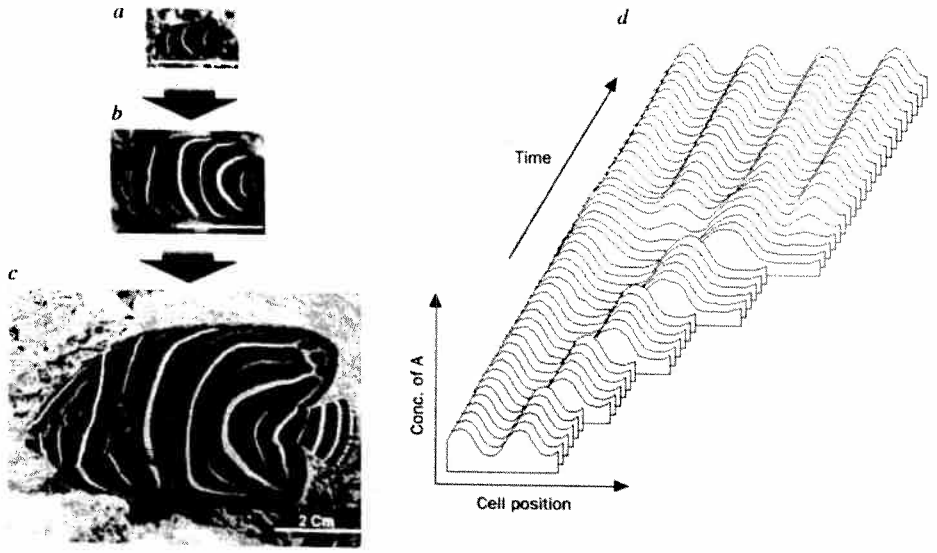

Fig. 1 Rearrangement of the stripe pattern of *Pomacanthus semicirculatus* and its computer simulation. **a-c**, Photographs of the juvenile of *P. semicirculatus*. Ages are approximately 2 months **(a)**, approximately 6 months **(b)** and approximately 12 months **(c)**. Scale bars, 2 cm. **d**, Computer simulation of the reaction-diffusion wave on the growing one-dimensional array of cells. One of the five cells is forced to duplicate periodically (once in 100 iterations). Concentration of activator is represented as the vertical height. The equations for calculation are as follows:

$$\frac{dA}{dt} = c_1A + c_2I + c_3 - D_A\frac{d^2A}{dx^2} - g_AA, \quad \frac{dI}{dt} = c_4A + c_5 - D_I\frac{d^2I}{dx^2} - g_II$$

where A and I are the concentration of the activator molecule and the inhibitor molecule, respectively, D_A and D_I are the diffusion constants, g_A and g_I are the decay constants, and $D_A = 0.007$, $D_I = 0.1$, $g_A = 0.03$, $g_I = 0.06$, $c_1 = 0.08$, $c_2 = 0.08$, $c_3 = 0.05$, $c_4 = 0.1$, $c_5 = 0.15$. Upper and lower limits for the synthesis rates of the activator ($c_1A + c_2I + c_3$) and inhibitor ($c_4A + c_5$) are set as $0 < c_1A + c_2I + c_3 < 0.18$ and $0 < c_4A + c_5 < 0.5$. These upper and lower limits are set to avoid unrealistic situations. A moderate upper-limit value of the activator synthesis rate is required to get a pattern of stripes rather than spots [15] (spots are obtained if this value is exceeded). We used the kinetics of Turing [1]. Other stripe-forming interactions [12, 15], in which the upper and lower limit is a natural outcome of the kinetics, can simulate the fish pattern rearrangement reported here.

The reaction-diffusion system used here consists of two hypothetical molecules (activator and inhibitor) which control the synthesis rate of each other. Figure 1(d) shows a computer simulation of a reaction-diffusion wave on a growing array of cells. At time 0, the field width is adjusted to be twice the intrinsic wavelength, calculated from the equations used in this simulation. One of the five cells is forced to duplicate periodically. As the field enlarges, all waves widen evenly. When the field length reaches about twice the original length, new peaks appear in the middle of the original peaks, as observed in *P. semicirculatus*, and the wavelength reverts to that of the original.

The juvenile of *P. imperator* has concentric stripes, which increase in number in a manner similar to that of *P. semicirculatus*. But when the *P. imperator* becomes an adult, the stripes become

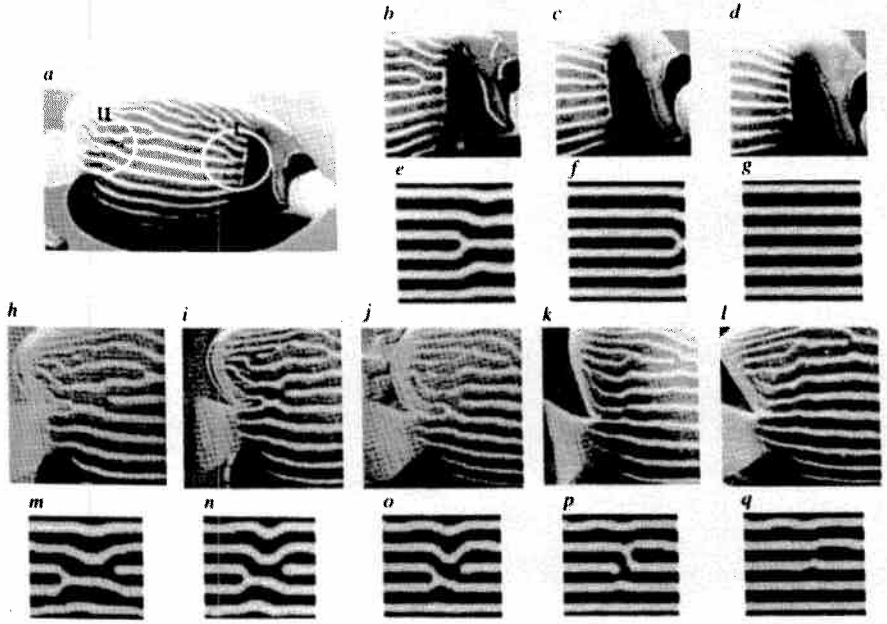

Fig. 2 Rearrangement of the stripe pattern of *Pomacanthus imperator* (horizontal movement of branching points) and its computer simulation. **a**, An adult *P. imperator* (approximately 10 months old). **b**, Close-up of region I in **a**. **c, d**, Photographs of region I of the same fish taken two (**c**) and three (**d**) months later. **e**, Starting stripe conformation for the simulation (region I). **f, g**, Results of the calculation after 30,000 (**f**) and 50,000 (**g**) iterations. **h**, Close-up of region II in **a**. **i-l**, Photographs of region II of the same fish taken 30 (**i**), 50 (**j**), 75 (**k**) and 90 (**l**) days later, respectively. **m**, Starting stripe conformation for the simulation (region II). **n-q**, Results of the calculation after 20,000 (**n**), 30,000 (**o**), 40,000 (**p**) and 50,000 (**q**) iterations, respectively. Fish (Fish World Co. Ltd (Osaka)) were maintained in artificial sea water (Martin Art, Senju). Skin patterns were recorded with a Canon video camera and printed by a Polaroid Slide Printer. In the simulated patterns, darker colour represents higher concentrations of the activator molecule. Equations and the values of the constants used, as Figure 1.

parallel to the anteroposterior axis by a process of continuous cutting and joining of the lines (data not shown). As they grow, the number of lines increases proportionally to body size, and the spaces between the lines are kept at an even width. The stripe pattern of *P. imperator* usually contains several branching points (Figure 2(a)). During growth, the branching points move horizontally like a zip, resulting in addition of new lines. Figure 2(b-d) shows a branching point moving in the anterior direction until it fuses with the border of the stripe region. In Figure 2(h-l), two branching points meet and disappear leaving a new line. This type of rearrangement also happens in the simulation of the reaction-diffusion system, by setting a homologous conformation as a starting pattern (Figure 2(e-g, m-q)). In Figure 2(e), the field height is adjusted to be six times the intrinsic wavelength. The waves in the right half are slightly extended, which causes loss of stability in this region. The rightward movement of the branch restores the stability of the righthand region. It is notable that not only the final conformation, but also each intermediate stage (Figure 2(n-p)), look quite similar to the actual pattern change that occurs in the fish (Figure 2(i-k)).

Branching points located on more dorsal or ventral regions behave differently. As shown in Figure 3(a-c), they move vertically by switching at a joint. This phenomenon can be simulated by the program used in Figure 1 and Figure 2 only by setting a different starting pattern (Figure 3(d-f)). In the simulation, a local region that contains a branching point is less stable than a region without a branch point, and joint switching tends to occur. The direction of joint switching is determined by the conformation of neighbouring lines. In our simulation, the line under the branching point is straighter than the line above. Because the curving line is less stable than the straight line, the joint switches in the upper direction. If both upper and lower lines are symmetrical to the branched line, horizontal movement of the branch point occurs (Figure 2). In the case of actual young fish, the lines in the middle region are usually straight, but in the dorsal and ventral regions the lines are curved. Branching points always move farther away from the middle region which consists of straight lines.

The times required for these pattern changes also suggest a mechanistic homology between actual fish and the simulations. In the simulation of joint switching, one change of joint can take place very quickly (in less than 1,000 iterations of calculation), because the change in pattern is quite local. For the horizontal movement of the branching point (from Figure 2(e to g)), more than 50,000 iterations are required because it is necessary for the upper lines and lower lines to 'slide' in order to evolve to a new pattern of stripes that are evenly spaced. In the case of real fish, the joint changes also occur quickly. In the fastest case we have observed, it took place in two days (data not shown), whereas the change from Figure 2(b to d) took more than three months.

Although we do not have any information about the molecules which are involved in the pattern-forming reaction, it is possible to estimate roughly the diffusion coefficients of the molecules by comparing the simulation and the actual pattern changing of fish stripe. The stripe spacing is approximately 0.5 cm in *P. imperator*, and approximately 10 grids in the simulated patterns (Figure 2); a grid in the simulation therefore represents 0.05 cm. The pattern change from Figure 2(h to l) took 90 days (7,776,000 seconds) in reality, and 50,000 iterations in the simulation. The time step for the simulation therefore corresponds to 155.5 seconds. These val-

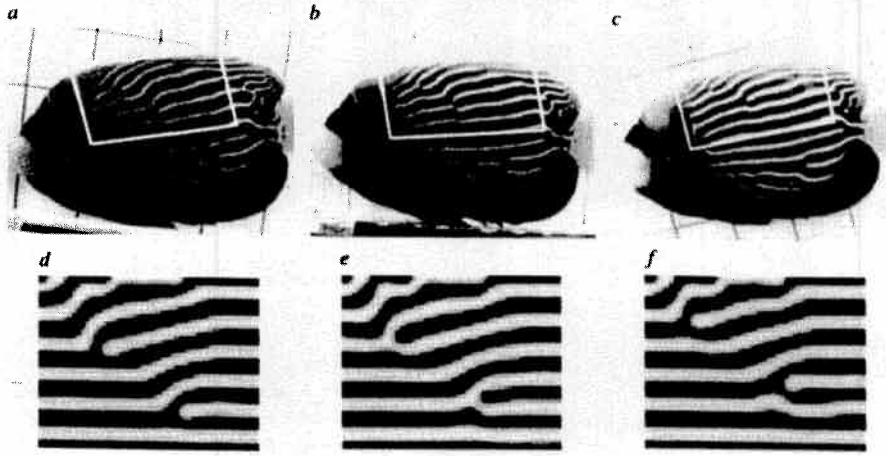

Fig. 3 Rearrangement of the stripe pattern of *P. imperator* (switch of joint) and its computer simulation. **a**, Photograph of a young *P. imperator* (approximately 7 months old). **b, c**, Photographs of the same fish taken 6 (**b**) and 12 (**c**) days later. **d**, Starting stripe conformation for the simulation. Pattern changing in the region surrounded by the white box was simulated. **e, f**, Results of the calculation after 2,000 (**e**) and 5,000 (**f**) iterations, respectively.

ues give diffusion coefficients of 1.125×10^{7} cm^2s^{-1} and $1.608 \times 10^{-6}cm^2s^{-1}$ for the activator and the inhibitor, respectively. Both values are in the range of the diffusion coefficients of proteins in aqueous media [9]. However, the diffusive molecules may be smaller than proteins, because the diffusion rate of molecules is usually much smaller in real biological systems than in aqueous media.

In some other biological systems, the insertion of new structures during growth have been observed and simulated [3, 10–14]. The novel features of the work reported here are that the inserted structure is a stripe and that the underlying mechanism is operative for a long period. The reaction-diffusion wave is a kind of standing wave. Therefore, to determine that a given pattern is consistent with a reaction-diffusion wave, it is necessary to impose some disturbance on the field and to see how the pattern responds. The pattern alteration of the *Pomacanthus*, accompanied by skin growth, can be taken as a natural experiment to help elucidate the underlying mechanisms which govern pattern formation. From the striking similarity between the actual and the simulated pattern alteration, it is highly probable that the mechanism is a reaction-diffusion system. Because the pattern-forming mechanism is maintained in adult skin, it should be possible to identify the molecules involved.

REFERENCES

1. A. M. Turing, *Phil. Trans. R. Soc.* **B237**, 37 (1952).
2. S. A. Kauffman, *Pattern Formation* (eds G. M. Malacinsky & S. Bryant.) 73–102 (Macmillan, New York, 1984).
3. H. Meinhardt, *Models of Biological Pattern Formation* (Academic, London, 1982).
4. J. D. Murray, *Scient. Am.* **258**, 80 (1988).
5. A. T. Winfree, *Nature* **352**, 568 (1991).
6. I. Lengyel & I. R. Epstein, *Science* **251**, 650 (1991).
7. Q. Ouyang & H. L. Swinney, *Nature* **352**, 610 (1991).
8. R. Pool, *Science* **251**, 627 (1991).
9. E. A. Dawes, *Quantitative Problems in Biology* (Longman, London, 1956).
10. E. Bunning & H. Z. Sagromsky, *Z. Naturf.* **B3**, 203 (1948).
11. T. C. Lacalli, *Phil. Trans. R. Soc.* **B294**, 547 (1981).
12. H. Meinhardt, *Rep. Progr. Phys.* **55**, 797 (1992).
13. L. A. Segel & J. L. Jackson, *J. theor. Biol* **37**, 545 (1972).
14. V. B. Wigglesworth, *J. exp. Biol.* **17**, 180 (1940).
15. H. Meinhardt, *Development* (suppl.) **107**, 169 (1989).

Letters to Nature

Nature, **380** (1996) 678.

T. Hofer and P. K. Maini
S. Kondo and R. Asai

SIR—Kondo and Asai [1] interpret observations on the time evolution of skin patterns of the angelfish (*Pomacanthus*) as the first instance of a Turing (reaction-diffusion) pattern in biology. But we believe that reaction-diffusion systems per se cannot provide a mechanistic basis for one of the main patterns reported in [1].

Reaction-diffusion systems are characterized by an intrinsic spatial wavelength of the self-organized concentration pattern, that is, the distance between adjacent peaks of chemical concentrations is determined solely by the system parameters (kinetic constants and diffusion coefficients). Although on a two-dimensional domain such as the fish skin, several equidistant geometrical arrangements of the concentration peaks are possible, the nonlinear terms of the reaction dynamics usually select only one of these possibilities—for the system chosen by Kondo and Asai, a regular array of stripes. These two features, an intrinsic wavelength and a strong tendency to form stripes, are the essential ingredients of the simulations they presented in [1]. Many pattern-forming systems other than reaction-diffusion are known which select an intrinsic spatial wavelength and pattern geometry [2], among them biologically relevant mechanisms involving chemotactic or haptotactic cell movement and mechanical forces [3]. Therefore, there is no justification for equating observed patterns with a particular mechanism, as suggested in [1].

Although our point does not exclude the possibility that a Turing system underlies the *Pomacanthus* skin patterns, we demonstrate here that its properties are not sufficient to explain perhaps the most striking observation of the paper, the regular insertion of new stripes between older ones during the growth of *Pomacanthus semicirculatus*. We have solved the authors' reaction-diffusion equations on a growing, two-dimensional domain—a more realistic representation of the fish skin than the one-dimensional domain used in [1].

Our results show that regular stripe-doubling sensitively depends on the artificial geometrical constraints of the one-dimensional domain (see Figure 1). As the restriction of one-dimensionality is removed, complete spatial rearrangement of the pattern occurs on the growing domain, which clearly is not seen in the fish. This behaviour is readily explained by the two properties of Turing systems emphasized above. As the domain grows bigger, new stripes should be added, one at a time, approximately conserving the spatial wavelength. Initially, the preexisting pattern appears to force a different sequence of stripe additions to occur, corresponding to the 'period-doubling' behaviour sometimes seen in one-dimensional systems [3].

Author affiliations: Thomas Hofer and Philip K. Maini: Centre for Mathematical Biology, Mathematical Institute, University of Oxford. Shigeru Kondo: Kyoto University Centre for Molecular Biology and Genetics, Kyoto, Japan. Rihito Asai: Kyoto University Seto Marine Biological Laboratory, Wakayama, Japan.

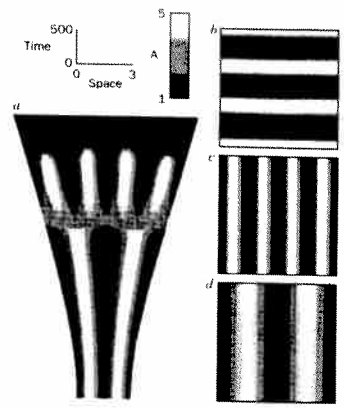

Fig. 1 Behaviour of the Turing system proposed in ref. 1 on a growing square domain (with the signs of the diffusion terms corrected). **a**, Concentration plot of A in a horizontal cross-section of the domain; time increases from bottom to top (see separate scales). The 4-stripe pattern produced by the first period-doubling is unstable, rearranges into a 3-stripe pattern perpendicular to the original pattern, and the stripe contours terminate. **b–d**, Snapshots of the stripe patterns corresponding to a (domains scaled to same size): **b**, initial 2-stripe pattern (t = 500); **c**, after period-doubling (t = 3,000); and **d**, after rearrangement into 3 stripes (2 + 2 half-stripes, t = 4,000, corresponding to the dark region in a). Simulations: equations scaled to the form $\partial u/\partial t = s^2 f(u) + D\nabla^2 u$, and solved with a standard ADI scheme on a fixed domain (mesh size 0.2, time step 0.05) with zero flux boundary conditions; increase in s is equivalent to increase in (domain length)^2 [2], here $s(t) = \sqrt{0.15 + 10^{-7}t^2}$. Patterning sequence is sensitive to the speed of domain growth and for faster growth rates the transitions become less controlled; we found transitions from 2 stripes to higher modes (5 stripes and more) with subsequent rearrangements.

However, this situation turns out to be unstable, and the whole pattern rearranges perpendicularly to the old one to form a new stripe pattern enlarged by one stripe. This behaviour does not depend on the aspect ratio of the domain; we have found complete perpendicular rearrangement of pattern even on very narrow (quasi-one-dimensional) domains. Thus, the patterning dynamics must involve an interplay of the mechanism that sets the distance between adjacent stripes and some form of 'memory' that conserves the location of old stripes. The 'memory' could be provided by pigment cells forming stable aggregations [4]. More specific quantitative models based on experimentally implicated mechanisms are needed to formulate testable predictions on the origin of the dynamic *Pomacanthus* skin patterns.

KONDO AND ASAI REPLY—With respect to Hofer and Maini's first criticism, we agree that many pattern-forming systems can explain the phenomenon we observed. These models have in common a set of interactions involving local activation/lateral inhibition coupled with the appropriate nonlinearities [5]. The most important message of our report [1] is that a dynamical mechanism like Turing's is viable for the fish patterns. It should therefore be possible to identify the real molecular mechanism by experiments. Of course, at present the details of the fish-patterning mechanism are unknown, and will not be understood until experiments are done.

Second, Hofer and Maini claim that a two-dimensional simulation of the *P. semicirculatus* pattern is more realistic than the one-dimensional simulation in our paper. This is by no means clear. All the stripe lines of *P. semicirculatus* are perpendicular to the body axis and there are no branch points. These features suggest the presence of a directional preference forcing the stripes to run in the same direction. A one-dimensional simulation captures some of the character of this system better than does an isotropic two-dimensional simulation.

REFERENCES

1. Kondo, S. & Asai, R. *Nature* **376**, 765–768 (1995).
2. Cross, M. C. & Hohenberg, P. C. *Rev. Mod. Phys.* **65**, 851–1112 (1993).
3. Murray, J. D. *Mathematical Biology* (Springer, Berlin, 1993).
4. Le Douarin, N. M. Curr. *Topics Dev. Biol.* **16**, 31–85 (1980).
5. Meinhardt, H. *Nature* **376**, 722–723 (1995).

READING 18.3

Complex Patterns in a Simple System

Commentary: For the purposes of this book, the point of this article is to illustrate the sorts of bizarre patterns that can arise with a pair of diffusion equations. The article considers functions $U(t, x, y)$ and $V(t, x, y)$, which are meant to represent the concentrations as functions of time t and space coordinates x and y of two different but interacting chemical species. Their time evolution is modeled by a pair of diffusion equations:

$$\frac{\partial}{\partial t}U = D_u\left(\frac{\partial^2}{\partial x^2}U + \frac{\partial^2}{\partial y^2}U\right) - UV^2 + F(1-U)$$
$$\frac{\partial}{\partial t}V = D_v\left(\frac{\partial^2}{\partial x^2}V + \frac{\partial^2}{\partial y^2}V\right) + UV^2 - (F+k)V.$$

[This is Eq. (2) in the article.] Here, D_u is the diffusion coefficient for U, and D_v the same for V. Meanwhile, F and k are constants. The author runs these equations on a computer and learns that his computer approximation to the true solutions produces bizarre patterns when D_u and D_v, F and k are chosen appropriately.

In any event, the equations above are t, x, y generalizations for two unknowns of our simpler, t, x diffusion equation $\frac{\partial}{\partial t}u = \mu\frac{\partial^2}{\partial x^2}u + ru$ for the one unknown u. (In the case of the paper, the term ru is replaced by a more complicated expression in U and V.)

Complex Patterns in a Simple System

Science, **261** (1993) 189–192.

John E. Pearson

Numerical simulations of a simple reaction-diffusion model reveal a surprising variety of irregular spatiotemporal patterns. These patterns arise in response to finite-amplitude perturbations. Some of them resemble the steady irregular patterns recently observed in thin gel reactor experiments. Others consist of spots that grow until they reach a critical size, at which time they divide in two. If in some region the spots become overcrowded, all of the spots in that region decay into the uniform background.

Patterns occur in nature at scales ranging from the developing *Drosophila* embryo to the large-scale structure of the universe. At the familiar mundane scales we see snow-flakes, cloud streets, and sand ripples. We see convective roll patterns in hydrodynamic experiments. We see regular and almost regular patterns in the concentrations of chemically reacting and diffusing systems [1]. As a consequence of the enormous range of scales over which pattern formation occurs, new pattern formation phenomenon is potentially of great scientific interest. In this report, I describe patterns recently observed in numerical experiments on a simple reaction-diffusion model. These patterns are unlike any that have been previously observed in theoretical or numerical studies.

The system is a variant of the autocatalytic Selkov model of glycolysis [2] and is due to Gray and Scott [3]. A variety of spatio-temporal patterns form in response to finite-amplitude perturbations. The response of this model to such perturbations was previously studied in one space dimension by Vastano *et al.* [4], who showed that steady spatial patterns could form even when the diffusion coefficients were equal. The response of the system in one space dimension is nontrivial and depends both on the control parameters and on the initial perturbation. It will be shown that the patterns that occur in two dimensions range from the well-known regular hexagons to irregular steady patterns similar to those recently observed by Lee *et al.* [5] to chaotic spatio-temporal patterns. For the ratio of diffusion coefficients used, there are no stable Turing patterns.

Most work in this field has focused on pattern formation from a spatially uniform state that is near the transition from linear stability to linear instability. With this restriction, standard bifurcation-theoretic tools such as amplitude equations have been developed and used with considerable success [6]. It is unclear whether the patterns presented in this report will yield to these now-standard technologies.

The Gray-Scott model corresponds to the following two reactions:

$$U + 2V \rightarrow 3V \qquad (1)$$
$$V \rightarrow P$$

Both reactions are irreversible, so P is an inert product. A nonequilibrium constraint is represented by a feed term for U. Both U and V are removed by the feed process. The resulting reaction-diffusion equations in dimensionless units are:

$$\frac{\partial U}{\partial t} = D_u\nabla^2 U - UV^2 + F(1-U)$$
$$\frac{\partial V}{\partial t} = D_u\nabla^2 V + UV^2 - (F+k)V \qquad (2)$$

where k is the dimensionless rate constant of the second reaction and F is the dimensionless feed rate. The system size is 2.5 by 2.5, and the diffusion coefficients are $D_u = 2\times10^{-5}$ and $D_v = 10^{-5}$. The

Author affiliation: John E. Pearson: Center for Nonlinear Studies, Los Alamos National Laboratory.

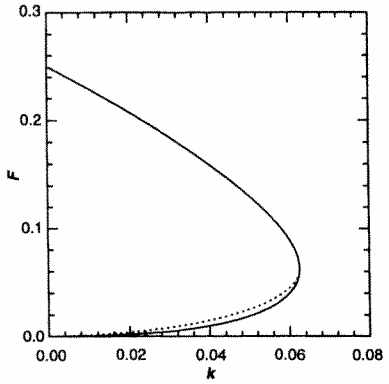

Fig. 1 Phase diagram of the reaction kinetics. Outside the region bounded by the solid line, there is a single spatially uniform state (called the trivial state) ($U = 1$, $V = 0$) that is stable for all (F, k). Inside the region bounded by the solid line, there are three spatially uniform steady states. Above the dotted line and below the solid line, the system is bistable: There are two linearly stable steady states in this region. As F is decreased through the dotted line, the nontrivial stable steady state loses stability through Hopf bifurcation. The bifurcating periodic orbit is stable for k less than 0.035 and unstable for k more than 0.035. No periodic orbits exist for parameter values outside the region bounded by the solid line.

boundary conditions are periodic. Before the numerical results are presented, consider the behavior of the reaction kinetics which are described by the ordinary differential equations that result upon dropping the diffusion terms in Eq. 2.

In the phase diagram shown in Figure 1, a trivial steady-state solution $U = 1$, $V = 0$ exists and is linearly stable for all positive F and k. In the region bounded above by the solid line and below by the dotted line, the system has two stable steady states. For fixed k, the nontrivial stable uniform solution loses stability through saddle-node bifurcation as F is increased through the upper solid line or by Hopf bifurcation to a periodic orbit as F is decreased through the dotted line. (For a discussion of bifurcation theory, see chapter 3 of [7].) In the case at hand, the bifurcating periodic solution is stable for k less than 0.035 and unstable for k more than 0.035. There are no periodic orbits for parameter values outside the region enclosed by the solid line. Outside this region the system is excitable. The trivial state is linearly stable and globally attracting. Small perturbations decay exponentially but larger perturbations result in a long excursion through phase space before the system returns to the trivial state.

The simulations are forward Euler integrations of the finite-difference equations resulting from discretization of the diffusion operator. The spatial mesh consists of 256 by 256 grid points. The time step used is 1. Spot checks made with meshes as large as 1024 by 1024 and time steps as small as 0.01 produced no qualitative difference in the results.

Initially, the entire system was placed in the trivial state ($U = 1$, $V = 0$). The 20 by 20 mesh point area located symmetrically about the center of the grid was then perturbed to ($U = 1/2$, $V = 1/4$). These conditions were then perturbed with ±1% random noise in order to break the square symmetry. The system was then integrated for 200,000 time steps and an image was saved. In all cases, the initial disturbance propagated outward from the central square, leaving patterns in its wake, until the entire grid was affected by the initial square perturbation. The propagation was wave-like, with the leading edge of the perturbation moving with an approximately constant velocity. Depending on the parameter values, it took on the order of 10,000 to 20,000 time steps for the initial perturbation to spread over the entire grid. The propagation velocity of the initial perturbation is thus on the order of

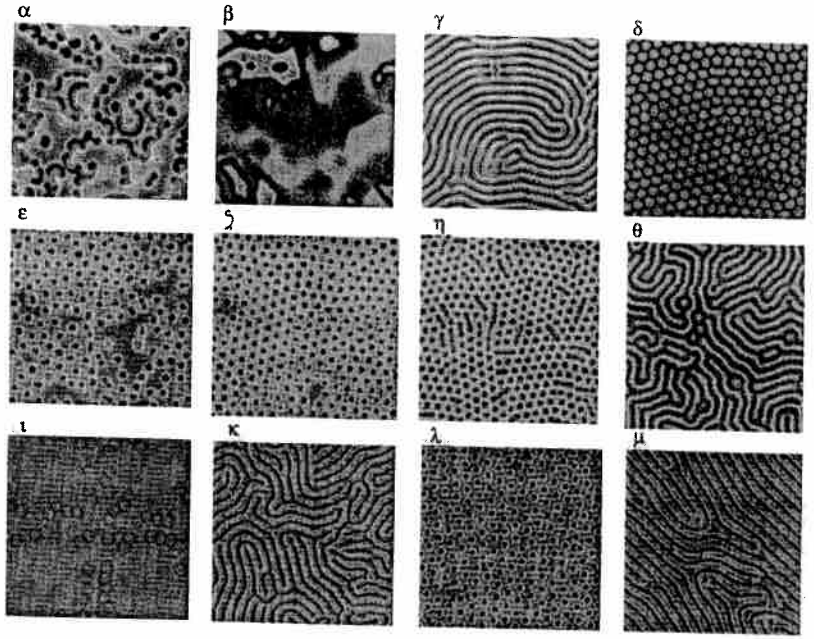

Fig. 2 The key to the map. The patterns shown in the figure are designated by Greek letters, which are used in Figure 3 to indicate the pattern found at a given point in parameter space.

1×10^{-4} space units per time unit. After the initial period during which the perturbation spread, the system went into an asymptotic state that was either time-independent or time-dependent, depending on the parameter values.

Figures 2 and 3 are phase diagrams; one can view Figure 3 as a map and Figure 2 as the key to the map. The 12 patterns illustrated in Figure 2 are designated by Greek letters. The color indicates the concentration of U with red representing $U = 1$ and blue representing $U \approx 0.2$; yellow is intermediate to red and blue. In Figure 3, the Greek characters indicate the pattern found at that point in parameter space. There are two additional symbols in Figure 3, R and B, indicating spatially uniform red and blue states, respectively. The red state corresponds to ($U = 1$, $V = 0$) and the blue state depends on the exact parameter values but corresponds roughly to ($U = 0.3$, $V = 0.25$).

Pattern α is time-dependent and consists of fledgling spirals that are constantly colliding and annihilating each other: full spirals never form. Pattern β is time-dependent and consists of what is generally called phase turbulence [8], which occurs in the vicinity of a Hopf bifurcation to a stable periodic orbit. The medium is unable to synchronize so the phase of the oscillators varies as a function of position. In the present case, the small-amplitude periodic orbit that bifurcates is unstable. Pattern γ is time-dependent. It consists primarily of stripes but there are small localized regions that oscillate with a relatively high frequency ($\approx 10^{-3}$). The active regions disappear, but new ones always appear elsewhere. In Figure 2 there is an active region near the top center of pattern γ. Pattern δ consists of regular hexagons except for apparently stable defects. Pattern η is time-dependent: a few of the stripes oscillate without apparent decay, but the remainder of the pattern remains time-independent. Pattern ι is time-dependent and was observed for only a single parameter value.

Patterns θ, κ, and μ resemble those observed by

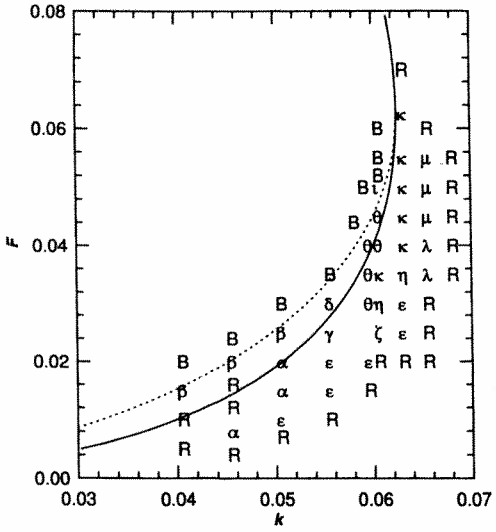

Fig. 3 The map. The Greek letters indicate the location in parameter space where the patterns in Figure 2 were found; *B* and *R* indicate that the system evolved to uniform blue and red states, respectively.

Lee *et al.* [5]. When blue waves collide, they stop, as do those observed by Lee *et al.* In pattern μ, long stripes grow in length. The growth is parallel to the stripes and takes place at the tips. If two distinct stripes that are both growing are pointed directly at each other, it is always observed that when the growing tips reach some critical separation distance, they alter their course so as not to collide. In patterns θ and κ, the perturbations grow radially outward with a velocity normal to the stripes. In these cases if two stripes collide, they simply stop, as do those observed by Lee *et al.* I have also observed, in one space dimension, fronts propagating toward each other that stop when they reach a critical separation. This is fundamentally new behavior for nonlinear waves that has recently been observed in other models as well [9].

Patterns ε, ζ, and λ share similarities. They consist of blue spots on a red or yellow background. Pattern λ is time-independent and patterns ε and ζ are time-dependent. Note that spots occur only in regions of parameter space where the system is excitable and the sole uniform steady state is the red state ($U = 1$, $V = 0$). Thus, the blue spots cannot persist for extended time unless there is a gradient present. Because the gradient is required for the existence of the spots, they must have a maximum size or there would be blue regions that were essentially gradient-free. Such regions would necessarily decay to the red state. Note that these gradients are self-sustaining and are not imposed externally. After the initial perturbation, the spots increase in number until they fill the system. This process is visually similar to cell division. After a spot has divided to form two spots, they move away from each other. During this period, each spot grows radially outward. The growth is a consequence of excitability. As the spots get further apart, they begin to elongate in the direction perpendicular to their motion. When a critical size is achieved, the gradient is no longer sufficient to maintain the center in the blue state, so the center decays to red, leaving two blue spots. This process is illustrated in Figure 4. Figure 4A was made just after the initial square perturbation had decayed to leave the four spots. In Figure 4B, the spots have moved away from each other and are beginning to elongate. In Figure 4C, the new spots are clearly visible. In Figure 4D, the replication process is complete. The subsequent evolution depends on the

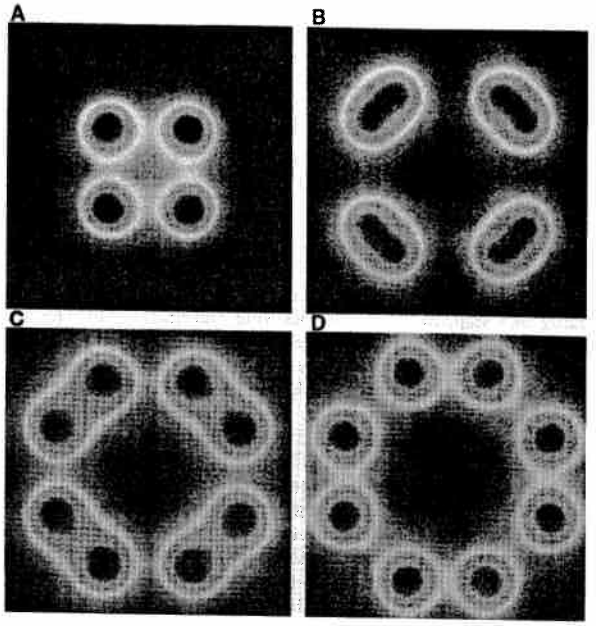

Fig. 4 Time evolution of spot multiplication. This figure was produced in a 256 by 256 simulation with physical dimensions of 0.5 by 0.5 and a time step of 0.01. The times t at which the figures were taken are as follows: **(A)** $t = 0$; **(B)** $t = 350$; **(C)** $t = 510$; and **(D)** $t = 650$.

control parameters. Pattern λ remains in a steady state. Pattern ζ remains time-dependent but with long-range spatial order except for local regions of activity. The active regions are not stationary. At any one instant, they do not appear qualitatively different from pattern ζ Fig. 2 but the location of the red disturbances changes with time. Pattern ε appears to have no long-range order either in time or space. Once the system is filled with blue spots, they can die due to overcrowding. This occurs when many spots are crowded together and the gradient over an extended region becomes too weak to support them. The spots in such a region will collapse nearly simultaneously to leave an irregular red hole. There are always more spots on the boundary of any hole, and after a few thousand time steps no sign of the hole will remain. The spots on its border will have filled it. Figure 5 illustrates this process.

Pattern ε is chaotic. The Liapunov exponent (which determines the rate of separation of nearby trajectories) is positive. The Liapunov time (the inverse of the Liapunov exponent) is 660 time steps, roughly equal to the time it takes for a spot to replicate, as shown in Figure 4. This time period is also about how long it takes for a molecule to diffuse across one of the spots. The time average of pattern epsilon is constant in space.

All of the patterns presented here arose in response to finite-amplitude perturbations. The ratio of diffusion coefficients used was 2. It is now well known that Turing instabilities that lead to spontaneous pattern formation cannot occur in systems in which all diffusion coefficients are equal. (For a comprehensive discussion of these issues, see Pearson and co-workers [10, 11]; for a discussion of Turing instabilities in the model at hand, see Vastano *et al.* [12].) The only Turing patterns that can occur bifurcate off the nontrivial steady uniform state (the blue state). Most of the patterns discussed in this report occur for parameter values such that the nontrivial steady state does not exist. With the ratio of diffusion coefficients used here, Turing pat-

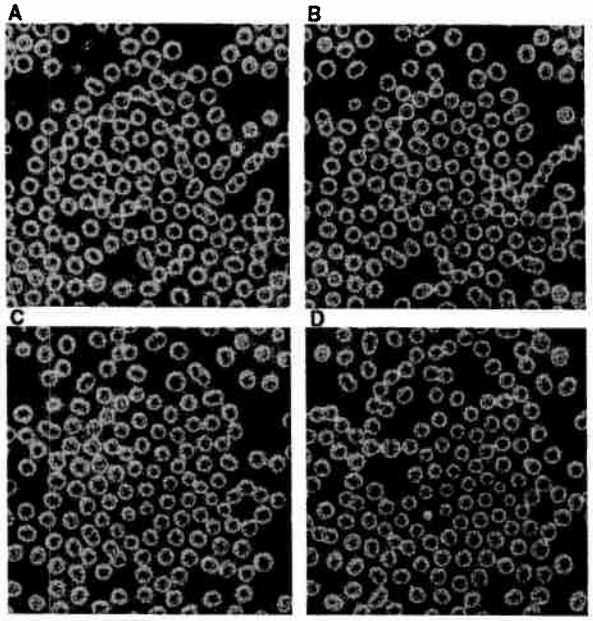

Fig. 5 Time evolution of pattern ε. The images are 250 time units apart. In the corners (which map to the same point in physical space), one can see a yellow region in (A) to (C). It has decayed to red in (D). In (A) and (B), the center of the left border has a red region that is nearly filled in (D).

terns occur only in a narrow parameter region in the vicinity of $F = k = 0.0625$, where the line of saddle-node bifurcations coalesces with the line of Hopf bifurcations. In the vicinity of this point, the branch of small-amplitude Turing patterns is unstable [12].

With equal diffusion coefficients, no patterns formed in which small asymmetries in the initial conditions were amplified by the dynamics. This observation can probably be understood in terms of the following fact: Nonlinear plane waves in two dimensions cannot be destabilized by diffusion in the case that all diffusion coefficients are equal [13]. During the initial stages of the evolution, the corners of the square perturbation are rounded off. The perturbation then evolves as a radial wave, either inward or outward depending on the parameter values. Such a wave cannot undergo spontaneous symmetry breaking unless the diffusion coefficients are unequal. However, I found symmetry breaking over a wide range of parameter values for a ratio of diffusion coefficients of 2. Such a ratio is physically reasonable even for small molecules in aqueous solution. Given this diffusion ratio and the wide range of parameters over which the replicating spot patterns exist, it is likely that they will soon be observed experimentally.

Recently Hasslacher et al. have demonstrated the plausibility of subcellular chemical patterns through lattice-gas simulations of the Selkov model [14]. The patterns discussed in the present article can also be found in lattice-gas simulations of the Selkov model and in simulations carried out in three space dimensions. Perhaps they are related to dynamical processes in the cell such as centrosome replication.

REFERENCES

1. G. Nicolis & I. Prigogine, *Self-Organization in Non-Equilibrium Systems* (Wiley, New York, 1977).

2. E. E. Selkov, *Eur. J. Biochem.* **4**, 79 (1968).
3. P. Gray & S. K. Scott, *Chem. Eng. Sci.* **38**, 29 (1983); *ibid.* **39**, 1087 (1984); *J. Phys. Chem.* **89**, 22 (1985).
4. J. A. Vastano, J. E. Pearson, W. Horsthemke & H. L. Swinney, *Phys. Lett. A* **124**, 6 (1987). *ibid.*, p. 7; *ibid.*, p. 320.
5. K. J. Lee, W. D. McCormick, Q. Ouyang & H. L. Swinney, *Science* **261**, 192 (1993).
6. P. Hohenberg & M. Cross, *Rev. Mod. Phys.* **65**, 3 (1993).
7. J. Guckenheimer & P. Holmes, *Nonlinear Oscillations, Dynamical Systems, and Bifurcations of Vector Fields* (Springer-Verlag, Berlin, 1983), chap. 3.
8. Y. Kuramoto, *Chemical Oscillations, Waves, and Turbulence* (Springer-Verlag, Berlin, 1984).
9. A. Kawczynski, W. Comstock & R. Field, *Physica D* **54**, 220 (1992); A. Hagberg & E. Meron, University of Arizona preprint.
10. J. E. Pearson & W. Horsthemke, *J. Chem. Phys.* **90**, 1588 (1989).
11. J. E. Pearson & W. J. Bruno, *Chaos* 2, 4 (1992); *ibid.*, p. 513.
12. J. A. Vastano, J. E. Pearson, W. Horsthemke & H. L. Swinney, *J. Chem. Phys.* **88**, 6175 (1988).
13. J. E. Pearson, *Los Alamos Publ.* LAUR 93-1758 (Los Alamos National Laboratory, Los Alamos, NM, 1993).
14. B. Hasslacher, R. Kapral & A. Lawniczak, *Chaos* **3**, 1 (1993).
15. I am happy to acknowledge useful conversations with S. Ponce-Dawson, W. Horsthemke, K. Lee, L. Segel, H. Swinney, B. Reynolds, and J. Theiler. I also thank the Los Alamos Advanced Computing Laboratory for the use of the Connection Machine and A. Chapman, C. Hansen, and P. Hinker for their ever-cheerful assistance with the figures.

READING 18.4

Direct and Continuous Assessment by Cells of Their Position in a Morphogen Gradient;
Activin Signalling and Response to a Morphogen Gradient

Commentary: A central question in biology is what determines the fate of cells in a developing embryo. For example, how do cells that become skin "know" they are to be skin, while those that become bone know that they are to be bone? Current belief has it that signaling molecules (called morphogens) are produced by certain cells and diffuse through the embryo. The morphogen concentration (or, more probably, concentrations of some number of morphogens) determines the cell fate by determining which genes become active. Of course, the signaling molecules are produced by cells which are 'told to do so' by the concentrations of other signaling molecules. Thus, there is a cascade of diffusable, chemical signals in the embryo that initiate gene activity at different times and places depending on their relative concentrations and timing of their appearance.

This article describes an experiment that determines that certain amphibian cells respond directly to changing morphogen concentrations in a "ratchet-like" manner. That is, the response of the cells is not a linear function of the morphogen concentration; rather it is a step function where a given response occurs when the morphogen concentration lies between two values, and when increased or decreased above or below these values, a distinctly different response occurs. The morphogen used here is a protein called Activin.

The term "gradient" in the title of this article and the next has the following interpretation: First, the term refers to the gradient of the function which measures the morphogen concentration. Second, the gradient of any function of some coordinates